



# Synthesis and Biological Evaluation of 5-Fluoro-2-Oxindole Derivatives as Potential $\alpha$ -Glucosidase Inhibitors

Jing Lin<sup>†</sup>, Qi-Ming Liang<sup>†</sup>, Yuan-Na Ye, Di Xiao, Li Lu, Meng-Yue Li, Jian-Ping Li, Yu-Fei Zhang, Zhuang Xiong\*, Na Feng\* and Chen Li\*

School of Biotechnology and Health Sciences, Wuyi University, Jiangmen, China

## OPEN ACCESS

### Edited by:

Shao-Hua Wang,  
Lanzhou University, China

### Reviewed by:

Wenneng Wu,  
Guiyang University, China  
Danying Huang,  
Guangdong University of  
Petrochemical Technology, China

### \*Correspondence:

Zhuang Xiong  
wyuchemxz@126.com  
Na Feng  
wyuchemfn@126.com  
Chen Li  
wyuchemlc@126.com

<sup>†</sup>These authors have contributed  
equally to this work

### Specialty section:

This article was submitted to  
Organic Chemistry,  
a section of the journal  
Frontiers in Chemistry

Received: 25 April 2022

Accepted: 09 May 2022

Published: 23 June 2022

### Citation:

Lin J, Liang Q-M, Ye Y-N, Xiao D, Lu L,  
Li M-Y, Li J-P, Zhang Y-F, Xiong Z,  
Feng N and Li C (2022) Synthesis and  
Biological Evaluation of 5-Fluoro-2-  
Oxindole Derivatives as Potential  $\alpha$ -  
Glucosidase Inhibitors.  
Front. Chem. 10:928295.  
doi: 10.3389/fchem.2022.928295

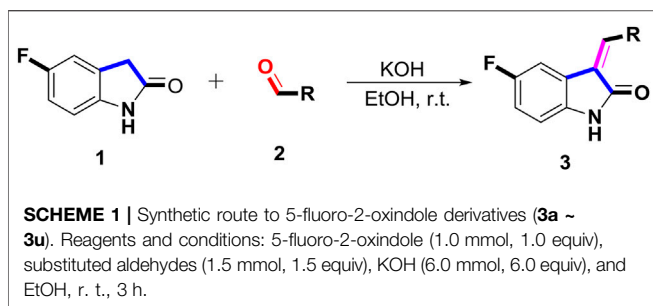
$\alpha$ -Glucosidase inhibitors are known to prevent the digestion of carbohydrates and reduce the impact of carbohydrates on blood glucose. To develop novel  $\alpha$ -glucosidase inhibitors, a series of 5-fluoro-2-oxindole derivatives (**3a** ~ **3v**) were synthesized, and their  $\alpha$ -glucosidase inhibitory activities were investigated. Biological assessment results showed that most synthesized compounds presented potential inhibition on  $\alpha$ -glucosidase. Among them, compounds **3d**, **3f**, and **3i** exhibited much better inhibitory activity with IC<sub>50</sub> values of 49.89 ± 1.16  $\mu$ M, 35.83 ± 0.98  $\mu$ M, and 56.87 ± 0.42  $\mu$ M, respectively, which were about 10 ~ 15 folds higher than acarbose (IC<sub>50</sub> = 569.43 ± 43.72  $\mu$ M). A kinetic mechanism study revealed that compounds **3d**, **3f**, and **3i** inhibited the  $\alpha$ -glucosidase in a reversible and mixed manner. Molecular docking was carried out to simulate the affinity between the compound and  $\alpha$ -glucosidase.

**Keywords:** oxindole,  $\alpha$ -glucosidase, inhibition, docking, kinetics

## 1 INTRODUCTION

Diabetes is a chronic metabolic disorder disease that increases the risk of cancer, stroke, peripheral arterial disease, cardiovascular disease, retinopathy, and kidney disease. (Wang et al., 2017; Sonia et al., 2019; Proença et al., 2019; Proença et al., 2017; Proença et al., 2018; Rocha et al., 2019; Santos et al., 2018; Wu et al., 2014; Wu et al., 2017). The prevalence of diabetes at all ages worldwide is rising. It is estimated that by 2030, the prevalence of diabetes may rise from 2.8% (171 million) in 2000 to 4.4% (366 million) (Zhong et al., 2019). Type 2 diabetes, which is characterized by insulin resistance, is the most common, which accounts for approximately 90% of all diabetic patients (Taha et al., 2015; Leong et al., 2019; Settypalli et al., 2019).

$\alpha$ -Glucosidase is an indispensable enzyme in the sugar metabolism pathway of organisms, and its main function is to hydrolyze glycosidic bonds into glucose (Chaudhry et al., 2019; Dan et al., 2019; Gollapalli et al., 2019; Krishna et al., 2019; Mendieta-Moctezuma et al., 2019; Spasov et al., 2019; Ye et al., 2019). Thus inhibiting the  $\alpha$ -glucosidase would obviously control the postprandial hyperglycemia.  $\alpha$ -Glucosidase inhibitors can block the hydrolysis of 1, 4-glycosidic bonds and delay the hydrolysis of carbohydrates into glucose, resulting in the effective reduction of postprandial blood sugar (Al-Salahi, et al., 2018; Qamar, et al., 2018; Shah, et al., 2018; Wang, et al., 2018). Up to now, a great number of naturally occurring and synthetic  $\alpha$ -glucosidase inhibitors have been reported. However, only several well-known inhibitors, such as acarbose, voglibose, and miglitol, are used clinically as first-line drugs. Moreover, these drugs have uncomfortable side effects (e.g., flatulence, abdominal pain, and diarrhea) (Taha et al., 2018a; Kasturi et al., 2018; Prachumart et al., 2018). These prompt us to develop effective and safe  $\alpha$ -glucosidase inhibitors from natural sources.



Lots of compounds from natural sources have shown potential inhibitory activity on  $\alpha$ -glucosidase. Oxindoles, the important indole-based derivatives, widely exist in many natural alkaloids. It

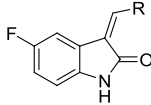
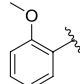
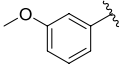
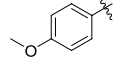
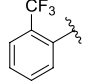
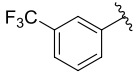
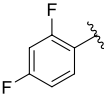
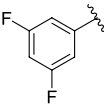
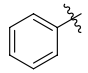
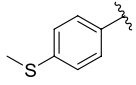
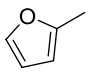
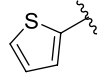
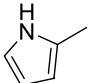
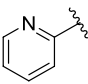
was reported that oxindoles have the ability to inhibit the  $\alpha$ -glucosidase (Khan et al., 2014; Asadollahi-Baboli and Dehnavi, 2018; Taha et al., 2018b). Moreover, oxindoles have attracted much attention due to their broad-spectrum biological activity, such as anti-inflammatory, anti-bacterial, and anti-tumor. (Yang et al., 2014; Xu et al., 2016; Alvarez et al., 2018; Bao et al., 2018; Huang et al., 2019). In addition, fluorine, a key atom in medicine, might enhance metabolic stability, improve the pharmacodynamic effect, and eliminate active metabolic intermediates (Johnson et al., 2020). Hence, 5-fluoro-2-oxindole was selected as the leading structure to synthesize the title compounds (**3a** ~ **3u**) through the condensation with the substituted aromatic aldehydes, followed by the screening on  $\alpha$ -glucosidase inhibitory activities and the molecular docking studies.

**TABLE 1** |  $\alpha$ -Glucosidase inhibitory activities of compounds (**3a** ~ **3v**).

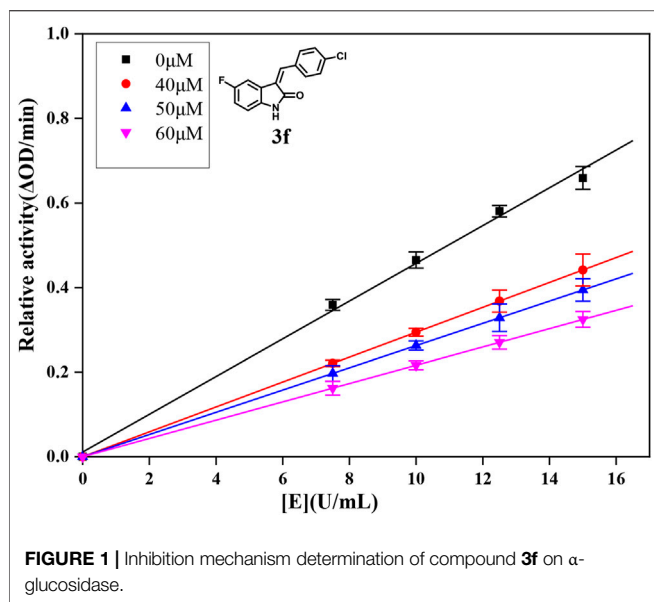
Compound	R	Inhibition rate at a concentration of 100 $\mu$ M (%)	IC <sub>50</sub> ( $\mu$ M)
<b>3a</b>		7.29 $\pm$ 0.16	>100 <sup>a</sup>
<b>3b</b>		5.19 $\pm$ 0.79	>100 <sup>a</sup>
<b>3c</b>		9.55 $\pm$ 0.13	>100 <sup>a</sup>
<b>3d</b>		89.19 $\pm$ 0.14	49.89 $\pm$ 1.16
<b>3e</b>		21.64 $\pm$ 0.78	>100 <sup>a</sup>
<b>3f</b>		90.52 $\pm$ 0.27	35.83 $\pm$ 0.98
<b>3g</b>		53.71 $\pm$ 0.47	95.68 $\pm$ 0.28
<b>3h</b>		31.61 $\pm$ 0.21	>100 <sup>a</sup>
<b>3i</b>		92.86 $\pm$ 0.32	56.87 $\pm$ 0.42

(Continued on following page)

**TABLE 1 |** (Continued)  $\alpha$ -Glucosidase inhibitory activities of compounds (**3a** ~ **3v**).

			
<b>3j</b>		$19.17 \pm 1.21$	$>100^a$
<b>3k</b>		$27.25 \pm 1.47$	$>100^a$
<b>3l</b>		$15.70 \pm 0.71$	$>100^a$
<b>3m</b>		$8.43 \pm 1.14$	$>100^a$
<b>3n</b>		$52.79 \pm 1.68$	$96.78 \pm 0.72$
<b>3o</b>		$18.78 \pm 1.15$	$>100^a$
<b>3p</b>		$55.89 \pm 1.71$	$92.62 \pm 0.45$
<b>3q</b>		$10.01 \pm 1.75$	$>100^a$
<b>3r</b>		$60.8 \pm 1.27$	$90.56 \pm 1.87$
<b>3s</b>		$4.49 \pm 1.88$	$>100^a$
<b>3t</b>		$5.67 \pm 1.11$	$>100^a$
<b>3u</b>		$3.77 \pm 1.35$	$>100^a$
<b>3v</b>		$3.99 \pm 1.28$	$>100^a$
<b>5-Fluoro-2-oxindole</b>			$(7.51 \pm 0.17) \times 10^3$
<b>Acarbose</b>			$569.43 \pm 43.72$

<sup>a</sup>The inhibitory activity of test compounds at 100  $\mu$ M is less than 50%.



## 2 RESULTS AND DISCUSSION

### 2.1 Chemistry

The 5-fluoro-2-oxindole derivatives (**3a** ~ **3v**) were prepared according to the synthetic route shown in **Scheme 1**. As the starting material, 5-fluoro-2-oxindole (**1**) was condensed with the substituted aromatic aldehydes (**2a** ~ **2v**) in the presence of KOH to produce the title compounds (**3a** ~ **3v**). The structures of compounds **3a** ~ **3v** were characterized by  $^1\text{H}$  NMR, MS, and melting point.

### 2.2 $\alpha$ -Glucosidase Inhibition Assay

$\alpha$ -Glucosidase from *Saccharomyces cerevisiae* (EC 3.2.1.20) was widely accepted and used to evaluate the inhibitory activity against  $\alpha$ -glucosidase. Then, the inhibitory activity of compounds (**3a** ~ **3v**) on  $\alpha$ -glucosidase from *S. cerevisiae* was investigated using *p*-NPG as the substrate. First, the inhibitory activities of compounds (**3a** ~ **3v**) were screened at a concentration of 100  $\mu\text{M}$ . As shown in **Table 1**, compounds **3d**, **3f**, and **3i** presented better activities, with inhibition of ~90% at a concentration of 100  $\mu\text{M}$  and those of compounds (**3g**, **3n**, **3p**, and **3r**) were ~50% at a concentration of 100  $\mu\text{M}$ , while those of other compounds were below 50% at a concentration of 100  $\mu\text{M}$ . Then,  $\text{IC}_{50}$  values of compounds **3d**, **3f**, **3i**, **3n**, **3p**, and **3r** were measured due to their better inhibitory activities. The  $\text{IC}_{50}$  values are summarized in **Table 1**, and the inhibitory activities of compounds **3d**, **3f**, and **3i** on  $\alpha$ -glucosidase are presented in **Figure 1**. For analyzing the inhibitory activities of compounds (**3a** ~ **3v**), the inhibitory activities of 5-fluoro-2-oxindole and acarbose were investigated. Among all compounds, compounds **3d**, **3f**, and **3i** exhibited much better potent inhibitory activity with  $\text{IC}_{50}$  values of  $56.87 \pm 0.42$   $\mu\text{M}$ ,  $49.89 \pm 1.16$   $\mu\text{M}$ , and  $35.83 \pm 0.98$   $\mu\text{M}$ , respectively, which were about 10 ~ 15 folds higher than that of acarbose ( $\text{IC}_{50} = 569.43 \pm 43.72$   $\mu\text{M}$ ) and significantly better than that of 5-fluoro-2-oxindole ( $\text{IC}_{50} = (7.51 \pm 0.17) \times 10^3$   $\mu\text{M}$ ).

### 2.3 Structure–Activity Relationships

Then, the structure–activity relationships of compounds (**3a** ~ **3v**) were analyzed according to the experimental data in **Table 1**. First, the steric effect of substituents at aldehydes was investigated based on the inhibitory activities of compounds **3a/3b/3c**, **3d/3e/3f**, **3g/3h/3i**, and **3m/3n**, with -F, -Cl, -Br, and -CF<sub>3</sub> at ortho-, meta- and para-positions of the benzene ring, and the order of the inhibitory activities is 4- > 2- > 3-. When the substituent was OCH<sub>3</sub> (**3j/3k/3l**), it turned out just the opposite. Second, the electronic effect of substituents was considered. The introduction of -F, -Cl, -Br, -CF<sub>3</sub>, and -OCH<sub>3</sub> at phenyl para-position (compounds **3c**, **3f**, **3i**, **3l**, and **3r**) could enhance the inhibitory activities with the inhibitory activity order of -Cl > -Br > -SCH<sub>3</sub> > -OCH<sub>3</sub> > -F. It could be seen that the inhibitory activity has no correlation with the steric and electronic effects of substituents at aldehydes. Furthermore, the introduction of various heterocycles (compounds **3s**, **3t**, **3u**, and **3v**) presented a negative effect on inhibitory activity. It could be concluded that the introduction of the substituents at the benzyl para-position of substituted aldehydes is beneficial to the improvement of the inhibitory activity. Therefore, the further derivatization of title compounds might be focused on the screening of substituents at the benzyl para-position of substituted aldehydes.

### 2.4 Inhibitory Mechanism Analysis

For further understanding the interaction mechanism of title compounds with  $\alpha$ -glucosidase, compounds **3d**, **3f**, and **3i** were selected to investigate the inhibition mechanism of  $\alpha$ -glucosidase through revealing the linkage between enzyme activity and the enzyme concentration in the presence of test compounds (figures for the inhibitory mechanism analysis of compounds **3f** was shown in **Figure 2** and figures for the inhibitory mechanism analysis of compounds **3d** and **3i** have been shown in the supporting information). The increasing concentrations of compounds **3d**, **3f**, or **3i** reduced the slope of the lines and the plots of the enzyme activity vs. the enzyme concentration at different concentrations of compounds **3d**, **3f**, or **3i** gave a group of straight lines, which all passed through the origin, indicating that the inhibitor reduces the activity of the enzyme and the inhibition of compounds **3d**, **3f**, or **3i** against  $\alpha$ -glucosidase was reversible.

In order to obtain the inhibition kinetics type of compounds **3d**, **3f**, and **3i**, the Lineweaver–Burk plot analysis method was carried out with different concentrations of test compounds and substrates. For compounds **3d**, **3f**, and **3i**, the plots of  $1/v$  vs.  $1/[S]$  gave a group of straight lines with different slopes that intersected the same point at the second quadrant, indicating that compounds **3d**, **3f**, and **3i** were mixed-type inhibitors. Then, the  $K_I$  values were calculated as 14.96, 33.85, and 22.72  $\mu\text{M}$ , respectively, and the  $K_{IS}$  values were calculated as 453.85, 58.31, and 24.74  $\mu\text{M}$ , respectively, which are summarized in **Table 2**. These results showed that compounds **3d**, **3f**, and **3i** could bind with the free enzyme as well as the enzyme–substrate complex of  $\alpha$ -glucosidase. In addition, the inhibition types of compounds **3d**, **3f**, and **3i**, different from that of acarbose, are the competitive inhibition type.

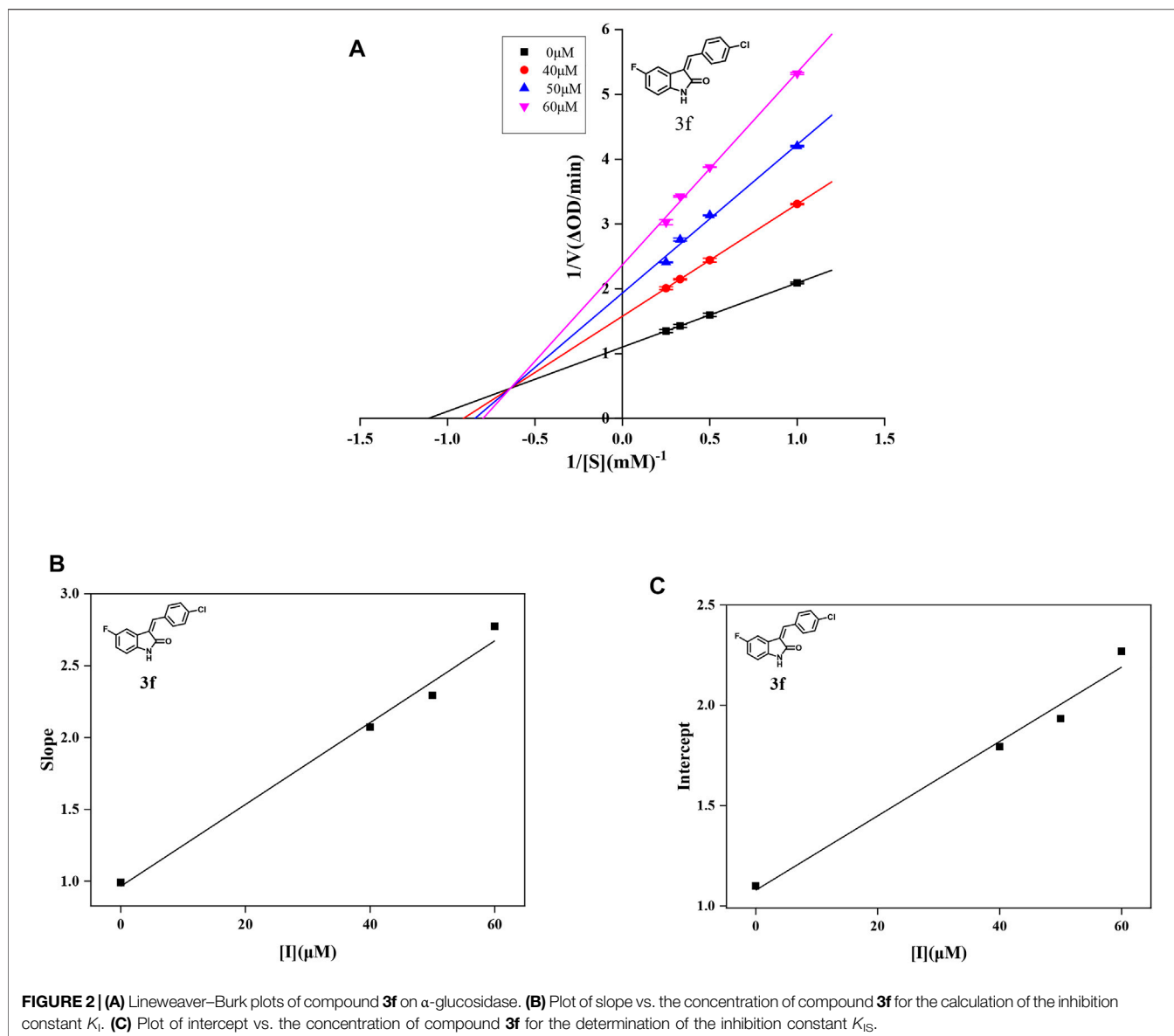


**TABLE 2 |** Type of inhibition mechanism and  $K_i$  and  $K_{IS}$  values of compounds **3d**, **3f**, and **3i**.

Compound	Inhibition mechanism	$K_i$ ( $\mu\text{M}$ )	$K_{IS}$ ( $\mu\text{M}$ )
<b>3d</b>	Mixed type	14.96	453.85
<b>3f</b>	Mixed type	33.85	58.31
<b>3i</b>	Mixed type	22.72	24.74

## 2.5 Molecular Docking Studies

With the purpose of acquiring a better comprehension of the mutual effects between compounds **3d**, **3f**, and **3i** and  $\alpha$ -glucosidase, molecular docking studies were implemented using Sybyl tools. The 3D structures of *S. cerevisiae*  $\alpha$ -glucosidase (EC 3.2.1.20) are unavailable, and oligo-1, 6-glucosidase from *S. cerevisiae* (PDB: 1UOK) was selected as

the target protein. Also, the sequence similarity is about 62.0% and the sequence identity is about 38.0%, as compared with  $\alpha$ -glucosidase. As demonstrated in **Figure 3A**, compounds **3d**, **3f**, and **3i** were well inserted into the active pocket of  $\alpha$ -glucosidase, with similar angles and positions. A hydrogen bond between carbonyl of compounds **3d**, **3f**, and **3i** and amino acid sequences of GLN330 was formed to increase the affinity with  $\alpha$ -glucosidase (**Figure 3B**). These similar integrated situations of compounds **3d**, **3f**, and **3i** with  $\alpha$ -glucosidase indicated the same inhibition mechanism. In addition, the lipophilic potential interaction between **3d**, **3f**, and **3i** and the active pocket was investigated. As shown in **Figure 3C**, the active pocket external is more lipophilic than the interior. Then, in **Figure 3D**, the fluorophenyl as the lipophilic fraction of **3d**, **3f**, and **3i** was close to the lipophilic potential region, while the pyrrole ring as the hydrophilic fraction was near to the hydrophilic region.

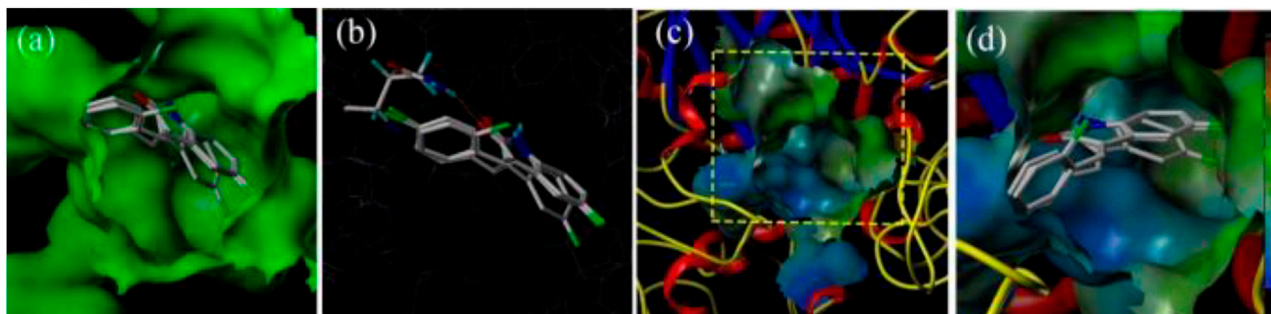


**FIGURE 3 | (A)** The insertion of compounds **3d**, **3f**, and **3i** into the active pocket of  $\alpha$ -glucosidase; **(B)** The hydrogen-bond interaction between carbonyl of the compounds (**3d**, **3f**, and **3i**) and  $\alpha$ -glucosidase; **(C)** The lipophilic interaction between the compounds (**3d**, **3f**, and **3i**) and  $\alpha$ -glucosidase; **(D)** The fluorophenyl as the lipophilic fraction of compounds **3d**, **3f**, and **3i** binding to  $\alpha$ -glucosidase.

## 3 EXPERIMENTAL

### 3.1 Chemicals

$\alpha$ -Glucosidase from *S. cerevisiae* (EC 3.2.1.20) and 4-nitrophenyl- $\beta$ -D-galactopyranoside (*p*-NPG) were supplied by Sigma-Aldrich. All other reagents were of analytical grade. The water used was re-distilled and ion-free.

### 3.2 Instruments

$^1\text{H}$  NMR was recorded by using a NMR spectrometer (DPX-500 MHz) in chloroform-*d* or DMSO-*d*<sub>6</sub>, with chemical shifts ( $\delta$ ) given in parts per million (ppm) relative to TMS as internal standard and recorded. Mass spectrometry was determined on a (LCQTM) LC-MS supplied by Thermo Fisher Scientific (Shanghai) Co., Ltd. Melting points were measured on a micro melting point instrument, which was supplied by Shanghai Yidian Physical Optical Instrument Co., Ltd. The absorbance was recorded using a microplate reader supplied by Thermo Fisher Scientific (Shanghai) Co., Ltd.

### 3.3 Synthesis of Compounds **3a** ~ **3v**

To a solution of **1** (1.0 mmol, 1.0 equiv.) and **2a** ~ **2v** in 10 ml absolute ethanol was added KOH (6 mmol, 6.0 equiv.), followed by the addition of the corresponding substituted aldehydes. Then, the mixture was stirred at room temperature for 3 h and detected to be complete by TLC. The mixture was adjusted to the pH value between 2.0 and 3.0, followed by the evaporation of ethanol, and extraction with ethyl acetate. The ethyl acetate layer was washed with saturated NaHCO<sub>3</sub> and brine and then was concentrated under vacuum to give the crude product, subsequently by the recrystallization with ethanol to give compounds **3a** ~ **3v**.

(*Z*)-5-Fluoro-3-(2-Fluorobenzylidene) Indolin-2-One (**3a**). Orange-yellow crystal; yield 65.0%; m p.: 228.3–230.2°C;  $^1\text{H}$  NMR (500 MHz, DMSO-*d*<sub>6</sub>)  $\delta$  10.73 (s, 1H), 7.77 (td, *J* = 7.7, 1.7 Hz, 1H), 7.65–7.55 (m, 2H), 7.47–7.36 (m, 2H), 7.13 (td, *J* = 9.0, 2.6 Hz, 1H), 6.94 (dd, *J* = 9.0, 2.6 Hz, 1H), and 6.88 (dd, *J* = 8.5, 4.6 Hz, 1H); HRMS (ESI) calculated for C<sub>15</sub>H<sub>9</sub>F<sub>2</sub>NO [M - H]<sup>-</sup>: m/z = 256.24, found 255.85.

(*Z*)-5-Fluoro-3-(3-Fluorobenzylidene) Indolin-2-One (**3b**). Orange-yellow crystal; yield 41.2%; m p.: 191.4–192.2°C;  $^1\text{H}$  NMR (500 MHz, chloroform-*d*)  $\delta$  7.81 (s, 1H), 7.49 (td, *J* = 8.0, 5.7 Hz, 1H), 7.42 (dp, *J* = 7.6, 0.9 Hz, 1H), 7.30 (ddd, *J* = 8.9, 6.8, 2.4 Hz, 2H), 7.20–7.15 (m, 1H), 6.97 (td, *J* = 8.7, 2.5 Hz, 1H), 6.82 (dd, *J* = 8.6, 4.4 Hz, 1H); HRMS (ESI) calculated for C<sub>15</sub>H<sub>9</sub>F<sub>2</sub>NO [M - H]<sup>-</sup>: m/z = 256.24, found 256.09.

(*Z*)-5-Fluoro-3-(4-Fluorobenzylidene) Indolin-2-One (**3c**). Orange-yellow crystal; yield 55.7%; mp.: 217.0–219.6°C;  $^1\text{H}$  NMR (500 MHz, chloroform-*d*)  $\delta$  8.10 (s, 1H), 7.82 (s, 1H), 7.64 (dd, *J* = 8.5, 5.4 Hz, 2H), 7.32 (dd, *J* = 9.1, 2.5 Hz, 1H), 7.20 (t, *J* = 8.4 Hz, 2H), 6.96 (td, *J* = 8.8, 2.6 Hz, 1H), and 6.83 (dd, *J* = 8.5, 4.4 Hz, 1H); HRMS (ESI) calculated for C<sub>15</sub>H<sub>9</sub>F<sub>2</sub>NO [M-H]<sup>-</sup>: m/z = 256.24, found 256.17.

(*Z*)-3-(2-Chlorobenzylidene)-5-Fluoroindolin-2-One (**3d**). Orange-yellow crystal; yield 82.4%; m p.: 219.7–221.9°C;  $^1\text{H}$  NMR (500 MHz, chloroform-*d*)  $\delta$  8.12 (s, 1H), 7.92 (s, 1H), 7.68 (dd, *J* = 7.5, 1.8 Hz, 1H), 7.54 (dd, *J* = 7.9, 1.4 Hz, 1H), 7.40 (dtd, *J* = 20.5, 7.5, 1.6 Hz, 2H), 7.04 (dd, *J* = 8.9, 2.6 Hz, 1H), 6.94 (td, *J* = 8.8, 2.6 Hz, 1H), and 6.82 (dd, *J* = 8.5, 4.3 Hz, 1H); HRMS (ESI) calculated for C<sub>15</sub>H<sub>9</sub>ClFNO [M-H]<sup>-</sup>: m/z = 272.69, found 271.96.

(*Z*)-3-(3-Chlorobenzylidene)-5-Fluoroindolin-2-One (**3e**). Orange-yellow crystal; yield 47.8%; mp: 237.4–238.9°C;  $^1\text{H}$  NMR (500 MHz, chloroform-*d*)  $\delta$  7.97 (s, 1H), 7.79 (s, 1H), 7.58 (dd, *J* = 2.1, 1.1 Hz, 1H), 7.54–7.50 (m, 1H), 7.46–7.43 (m, 2H), 7.25 (d, *J* = 2.5 Hz, 1H), 6.97 (td, *J* = 8.7, 2.6 Hz, 1H), and 6.82 (dd, *J* = 8.5, 4.4 Hz, 1H); HRMS (ESI) calculated for C<sub>15</sub>H<sub>9</sub>ClFNO [M-H]<sup>-</sup>: m/z = 272.69, found 272.10.

(*Z*)-3-(4-Chlorobenzylidene)-5-Fluoroindolin-2-One (**3f**). Orange-yellow crystal; yield 44.2%; mp: 200.6–202.5°C;  $^1\text{H}$  NMR (500 MHz, chloroform-*d*)  $\delta$  7.80 (s, 1H), 7.58 (d, *J* = 8.3 Hz, 2H), 7.51–7.45 (m, 2H), 7.30 (dd, *J* = 8.9, 2.5 Hz, 1H), 6.96 (td, *J* = 8.7, 2.6 Hz, 1H), and 6.82 (dd, *J* = 8.5, 4.4 Hz, 1H); HRMS (ESI) calculated for C<sub>15</sub>H<sub>9</sub>ClFNO [M-H]<sup>-</sup>: m/z = 272.69, found 272.39.

(*Z*)-3-(2-Bromobenzylidene)-5-Fluoroindolin-2-One (**3g**). Orange-yellow crystal; yield 69.7%; mp: 194.9–197.1°C;  $^1\text{H}$  NMR (500 MHz, chloroform-*d*)  $\delta$  7.90–7.82 (m, 1H), 7.73 (dd, *J* = 8.1, 1.1 Hz, 1H), 7.66 (dt, *J* =

7.7, 1.9 Hz, 1H), 7.44 (td,  $J = 7.4, 1.1$  Hz, 1H), 7.34 (td,  $J = 7.7, 1.6$  Hz, 1H), 7.00 (dd,  $J = 8.9, 2.6$  Hz, 1H), and 6.94 (td,  $J = 8.7, 2.6$  Hz, 1H); HRMS (ESI) calculated for  $C_{15}H_9BrFNO$   $[M + Na]^+$ :  $m/z = 340.15$ , found 340.59.

(Z)-3-(3-Bromobenzylidene)-

5-Fluoroindolin-2-One (3h). Orange-yellow crystal; yield 70.4%; mp: 222.6–223.8°C;  $^1H$  NMR (500 MHz, chloroform- $d$ )  $\delta$  8.31 (s, 1H), 7.86–7.67 (m, 2H), 7.66–7.48 (m, 2H), 7.38 (t,  $J = 7.9$  Hz, 1H), 7.24 (d,  $J = 2.6$  Hz, 1H), 6.97 (td,  $J = 8.7, 2.6$  Hz, 1H), and 6.84 (dd,  $J = 8.5, 4.4$  Hz, 1H); HRMS (ESI) calculated for  $C_{15}H_9BrFNO$   $[M + Na]^+$ :  $m/z = 357.15$ , found 357.97.

(Z)-3-(4-Bromobenzylidene)

-5-Fluoroindolin-2-One (3i). Orange-yellow crystal; yield 65.7%; mp: 249.3–251.6°C;  $^1H$  NMR (500 MHz, chloroform- $d$ )  $\delta$  7.77 (s, 1H), 7.67–7.61 (m, 2H), 7.51 (d,  $J = 8.4$  Hz, 2H), 7.30 (dd,  $J = 9.0, 2.6$  Hz, 1H), 6.96 (td,  $J = 8.7, 2.6$  Hz, 1H), and 6.81 (dd,  $J = 8.5, 4.4$  Hz, 1H); HRMS (ESI) calculated for  $C_{15}H_9BrFNO$   $[M + Na]^+$ :  $m/z = 341.15$ , found 340.97.

(Z)-5-Fluoro-3-(2-Methoxybenzylidene) Indolin-2-One (3j). Orange-yellow crystal; yield 52.7%; mp: 227.1–227.8°C;  $^1H$  NMR (500 MHz, chloroform- $d$ )  $\delta$  8.02 (s, 1H), 7.97 (s, 1H), 7.67 (dd,  $J = 7.7, 1.7$  Hz, 1H), 7.49–7.42 (m, 1H), 7.28 (dd,  $J = 9.2, 2.7$  Hz, 1H), 7.06 (td,  $J = 7.5, 1.0$  Hz, 1H), 7.00 (dd,  $J = 8.3, 1.0$  Hz, 1H), 6.91 (td,  $J = 8.8, 2.6$  Hz, 1H), 6.80 (dd,  $J = 8.5, 4.4$  Hz, 1H), and 3.89 (s, 3H); HRMS (ESI) calculated for  $C_{16}H_{12}FNO_2$   $[M-H]^-$ :  $m/z = 268.28$ , found 268.19.

(Z)-5-Fluoro-3-(3-Methoxybenzylidene) Indolin-2-One (3k). Orange-yellow crystal; yield 73.3%; mp: 200.1–202.1°C;  $^1H$  NMR (500 MHz, chloroform- $d$ )  $\delta$  7.86 (s, 1H), 7.45–7.38 (m, 2H), 7.23 (d,  $J = 7.5$  Hz, 1H), 7.14 (t,  $J = 2.0$  Hz, 1H), 7.04–6.90 (m, 2H), 6.82 (dd,  $J = 8.6, 4.4$  Hz, 1H), and 3.86 (s, 3H); HRMS (ESI) calculated for  $C_{16}H_{12}FNO_2$   $[M-H]^-$ :  $m/z = 268.28$ , found 268.01.

(Z)-5-Fluoro-3-(4-Methoxybenzylidene) Indolin-2-One (3l). Orange-yellow crystal; yield 42.8%; mp: 358.8–359.9°C;  $^1H$  NMR (500 MHz, chloroform- $d$ )  $\delta$  7.84 (s, 1H), 7.68–7.62 (m, 2H), 7.49 (dd,  $J = 9.3, 2.6$  Hz, 1H), 7.04–7.00 (m, 2H), 6.93 (dd,  $J = 8.8, 2.6$  Hz, 1H), 6.83 (dt,  $J = 9.0, 3.6$  Hz, 1H), and 3.91 (s, 3H); HRMS (ESI) calculated for  $C_{16}H_{12}FNO_2$   $[M-H]^-$ :  $m/z = 268.28$ , found 268.11.

(Z)-5-Fluoro-3-[2-(Trifluoromethyl) Benzylidene] Indolin-2-One (3m). Orange-yellow crystal; yield 53.1%; mp: 235.2–236.4°C;  $^1H$  NMR (500 MHz, chloroform- $d$ )  $\delta$  8.33–8.22 (m, 1H), 8.01 (q,  $J = 2.5$  Hz, 1H), 7.83 (d,  $J = 7.8$  Hz, 1H), 7.70–7.65 (m, 2H), 7.63–7.55 (m, 1H), 6.93 (td,  $J = 8.8, 2.6$  Hz, 1H), 6.83 (dd,  $J = 8.5, 4.3$  Hz, 1H), and 6.66 (dd,  $J = 8.7, 2.6$  Hz, 1H); HRMS (ESI) calculated for  $C_{16}H_9F_4NO$   $[M-H]^-$ :  $m/z = 306.25$ , found 305.91.

(Z)-5-Fluoro-3-[3-(Trifluoromethyl) Benzylidene] Indolin-2-One (3n). Orange-yellow crystal; yield 42.9%; mp: 199.7–200.5°C;  $^1H$  NMR (500 MHz, chloroform- $d$ )  $\delta$  7.87 (s, 1H), 7.85 (s, 1H), 7.81 (d,  $J = 7.7$  Hz, 1H), 7.73 (d,  $J = 7.8$  Hz, 1H), 7.64 (t,  $J = 7.8$  Hz, 1H), 7.18 (dd,  $J = 8.9, 2.6$  Hz, 1H), 6.97 (td,  $J = 8.7, 2.6$  Hz, 1H), and 6.83 (dd,  $J = 8.6, 4.3$  Hz, 1H); HRMS (ESI) calculated for  $C_{16}H_9F_4NO$   $[M-H]^-$ :  $m/z = 306.25$ , found 306.01.

(Z)-3-(2,4-Difluorobenzylidene)

-5-Fluoroindolin-2-One (3o). Orange-yellow crystal; yield 55.3%; mp: 221.1–224.3°C;  $^1H$  NMR (500 MHz, chloroform- $d$ )  $\delta$  8.31–8.21 (s, 1H), 8.01 (s, 1H), 7.83 (d,  $J = 7.8$  Hz, 1H), 7.68–7.65 (m, 2H), 7.62–7.58 (m, 1H), 6.93 (td,  $J = 8.8, 2.6$  Hz, 1H), 6.83 (dd,  $J = 8.5, 4.3$  Hz, 1H), and 6.66 (dd,  $J = 8.7, 2.6$  Hz, 1H); HRMS (ESI) calculated for  $C_{16}H_9F_4NO$   $[M + H]^+$ :  $m/z = 276.23$ , found 278.01.

(Z)-3-(3,4-Difluorobenzylidene)-

5-Fluoroindolin-2-One (3p). Orange-yellow crystal; yield 44.6%; mp: 189.2–190.2°C;  $^1H$  NMR (500 MHz, chloroform- $d$ )  $\delta$  8.99 (dd,  $J = 10.1, 2.7$  Hz, 1H), 8.91 (ddd,  $J = 4.6, 2.0, 0.8$  Hz, 1H), 7.83 (td,  $J = 7.7, 1.9$  Hz, 1H), 7.73 (s, 1H), 7.63 (dd,  $J = 7.7, 1.1$  Hz, 1H), 7.36 (ddd,  $J = 7.7, 4.7, 1.1$  Hz, 1H), 7.01 (td,  $J = 8.6, 2.7$  Hz, 1H), and 6.80 (dd,  $J = 8.5, 4.4$  Hz, 1H); HRMS (ESI) calculated for  $C_{15}H_8F_3NO$   $[M-H]^-$ :  $m/z = 274.23$ , found 274.02.

(Z)-3-Benzylidene-5-Fluoroindolin-2-One (3q). Orange-yellow crystal; yield 76.3%; mp: 198.9–199.7°C;  $^1H$  NMR (500 MHz, chloroform- $d$ )  $\delta$  8.93 (s, 1H), 7.90 (s, 1H), 7.67–7.62 (m, 2H), 7.53–7.46 (m, 3H), 7.36 (dd,  $J = 9.1, 2.6$  Hz, 1H), 6.94 (td,  $J = 8.7, 2.5$  Hz, 1H), and 6.86 (dd,  $J = 8.5, 4.5$  Hz, 1H); HRMS (ESI) calculated for  $C_{15}H_8F_3NO$   $[M-H]^-$ :  $m/z = 238.25$ , found 237.99.

(Z)-5-Fluoro-3-[4-(Methylthio) Benzylidene] Indolin-2-One (3r). Orange-yellow crystal; yield 41.8%; mp: 246.1–247.1°C;  $^1H$  NMR (500 MHz, chloroform- $d$ )  $\delta$  8.13 (s, 1H), 7.81 (s, 1H), 7.61–7.55 (m, 2H), 7.44 (dd,  $J = 9.0, 2.6$  Hz, 1H), 7.36–7.31 (m, 2H), 6.94 (td,  $J = 8.7, 2.5$  Hz, 1H), 6.82 (dd,  $J = 8.5, 4.4$  Hz, 1H), and 2.56 (s, 3H); HRMS (ESI) calculated for  $C_{16}H_{12}FNOS$   $[M-H]^-$ :  $m/z = 284.34$ , found 284.13.

(Z)-5-Fluoro-3-(Furan-2-ylmethylene) Indolin-2-One (3s). Orange-yellow crystal; yield 72.5%; mp: 237.9–238.8°C;  $^1H$  NMR (500 MHz, chloroform- $d$ )  $\delta$  7.76 (s, 1H), 7.41 (s, 1H), 7.24–7.16 (m, 2H), 6.88 (td,  $J = 8.8, 2.5$  Hz, 1H), 6.82 (dd,  $J = 8.5, 4.2$  Hz, 2H), and 6.42 (dt,  $J = 4.0, 2.1$  Hz, 1H); HRMS (ESI) calculated for  $C_{16}H_{12}FNOS$   $[M-H]^-$ :  $m/z = 228.21$ , found 227.95.

(Z)-5-Fluoro-3-(Thiophen-2-ylmethylene) Indolin-2-One (3t). Orange-yellow crystal; yield 44.6%; mp: 219.0–223.4°C;  $^1H$  NMR (500 MHz, chloroform- $d$ )  $\delta$  8.01 (dd,  $J = 9.4, 2.5$  Hz, 1H), 7.97 (s, 1H), 7.85 (s, 1H), 7.65 (dd,  $J = 23.4, 4.4$  Hz, 2H), 7.23 (dd,  $J = 5.1, 3.7$  Hz, 1H), 6.99 (td,  $J = 8.7, 2.5$  Hz, 1H), and 6.84 (dd,  $J = 8.5, 4.5$  Hz, 1H); HRMS (ESI) calculated for  $C_{16}H_{12}FNOS$   $[M-H]^-$ :  $m/z = 244.27$ , found 244.14.

(Z)-3-[(1H-Pyrrol-2-yl)methylene]-5-Fluoroindolin-2-One (3u). Orange-yellow crystal; yield 54.4%; mp: 198.9–201.6°C;  $^1H$  NMR (500 MHz, chloroform- $d$ )  $\delta$  13.30 (s, 1H), 7.76 (s, 1H), 7.41 (s, 1H), 7.22 (s, 1H), 7.19 (dd,  $J = 8.7, 2.5$  Hz, 1H), 6.88 (td,  $J = 8.8, 2.5$  Hz, 1H), 6.82 (d,  $J = 4.2$  Hz, 2H), and 6.42 (dt,  $J = 4.0, 2.1$  Hz, 1H); HRMS (ESI) calculated for  $C_{13}H_9FN_2O$   $[M-H]^-$ :  $m/z = 227.23$ , found 227.02.

(Z)-5-Fluoro-3-(Pyridin-2-ylmethylene) Indolin-2-One (3v). Orange-yellow crystal; yield 47.9%; mp: 248.5–251.2°C;  $^1H$  NMR (500 MHz, chloroform- $d$ )  $\delta$  8.99 (dd,  $J = 10.1, 2.7$  Hz, 1H), 8.91 (ddd,  $J = 4.6, 2.0, 0.8$  Hz, 1H), 7.83 (td,  $J = 7.7, 1.9$  Hz, 1H), 7.73 (s, 1H), 7.63 (dd,  $J = 7.7, 1.1$  Hz, 1H), 7.36 (ddd,  $J = 7.7, 4.7, 1.1$  Hz, 1H), 7.01 (td,  $J = 8.6, 2.7$  Hz, 1H), and 6.80 (dd,  $J = 8.5, 4.4$  Hz, 1H); HRMS (ESI) calculated for  $C_{13}H_9FN_2O$   $[M-H]^-$ :  $m/z = 239.24$ , found 238.93.

### 3.4 $\alpha$ -Glucosidase Inhibitory Assay

The  $\alpha$ -glucosidase inhibition of synthetic compounds was performed as previously reported methods with minor modification (Deng et al., 2022) which is as follows: briefly, 130  $\mu$ l of phosphate buffer (10 mM, pH 6.8), 10  $\mu$ l of  $\alpha$ -glucosidase (1 U/ml), and 10  $\mu$ l of test compound solution were added into the wells of a 96-well plate, followed by incubation for 10 min at 37°C. Then, 50  $\mu$ l of *p*-NPG (1 mM) was added, and the plate was further incubated for 30 min at 37°C. Finally, the absorbance of each well was recorded at 405 nm using a microplate reader. Acarbose was used as the reference. The inhibition of the test compound on  $\alpha$ -glucosidase was calculated as follows: inhibition ratio (%) = [(A - B)/A]  $\times$  100, where A is the absorbance of blank and B is the absorbance of the test compound. Each concentration was experimented four times in parallel. Half inhibitory concentration (IC<sub>50</sub>) was obtained from the fitting curve of inhibition ratio vs. test compound with different concentrations.

### 3.5 Kinetics Mechanism Analysis

Compounds **3d**, **3f**, and **3i** with much better  $\alpha$ -glucosidase inhibitory activity were selected for kinetic analysis. The experiments were performed to investigate the kinetics mechanism of compounds **3d**, **3f**, and **3i** by the previously reported method (Xu et al., 2019). To determine the inhibition mechanism, the final concentrations for **3d** were 0, 40, 50, 60  $\mu$ M, for **3f** were 0, 40, 50, 60  $\mu$ M, and for **3i** were 0, 30, 40, 50  $\mu$ M, the final substrate *p*-NPG concentration was 0.25 mM, and the final concentrations for  $\alpha$ -glucosidase were  $3.75 \times 10^{-2}$ ,  $5.00 \times 10^{-2}$ ,  $6.25 \times 10^{-2}$ , and  $7.50 \times 10^{-2}$  U/ml. Then, the inhibition rates were measured by the aforementioned method.

To analyze the inhibition type, the final concentrations for **3d** were 0, 40, 50, and 60  $\mu$ M, for **3f** were 0, 40, 50, and 60  $\mu$ M, and for **3i** were 0, 30, 40, and 50  $\mu$ M, the final  $\alpha$ -glucosidase concentration was  $5.00 \times 10^{-2}$  U/ml, and final concentrations for substrate *p*-NPG concentration were 0.25, 0.50, 0.75, and 1.00 mM. The inhibition rates were obtained by the aforementioned method. The inhibition type on  $\alpha$ -glucosidase was analyzed by using Lineweaver–Burk plots of the inverse of velocities (1/v) vs. the inverse of substrate concentration 1/[S]. The  $K_I$  and  $K_{IS}$  were obtained from the slope and the vertical intercept vs. the inhibitor concentration, respectively.

### 3.6 Molecular Docking

The molecular docking between compounds **3d**, **3f**, and **3i** and  $\alpha$ -glucosidase were simulated with Sybyl-2.1.1 (Tripos, Shanghai, China) (Hu et al., 2021). First, compounds **3d**, **3f**, and **3i** were prepared by hydrogenation and energy minimization using the MM2 program. In the energy minimization program, the energy convergence criterion was revised to 0.001 kcal/mol, optimizing the energy gradient that was revised to 2,500 times, and the charge was run with the Gasteiger–Hückle charges method. Next, after being retrieved from the RCSB Protein Database (PDB: 1UOK), the  $\alpha$ -glucosidase structure was prepared, followed by the procedure of removing water, termini treatment, adding

hydrogens, adding charges with the MMFF94, fixing side chain amides, and staged minimization. The active pocket of  $\alpha$ -glucosidase was generated with the automatic mode. Then, the molecular docking between compounds **3d**, **3f**, and **3i** and  $\alpha$ -glucosidase were operated in the default format.

## 4 CONCLUSION

In summary, a series of  $\alpha$ -glucosidase inhibitors based on 5-fluoro-2-oxindole have been synthesized and evaluated. Most synthesized compounds presented better potential inhibitory on  $\alpha$ -glucosidase than the parent compound. Among them, compounds **3d**, **3f**, and **3i** exhibited much better inhibitory activity with IC<sub>50</sub> values of  $49.89 \pm 1.16$ ,  $35.83 \pm 0.98$  and  $56.87 \pm 0.42$   $\mu$ M, respectively, which were about 10 ~ 15 folds higher activities than acarbose (IC<sub>50</sub> =  $569.43 \pm 43.72$   $\mu$ M) that was used as reference. The kinetics mechanism study revealed that compounds **3d**, **3f**, and **3i** inhibited the  $\alpha$ -glucosidase in a reversible and mixed manner. Molecular docking confirmed that compounds could effectively integrate with  $\alpha$ -glucosidase. These results indicated that these synthesized compounds could be used as the leading structure in the research and development of  $\alpha$ -glucosidase inhibitors for the prevention and treatment of type 2 diabetes.

## DATA AVAILABILITY STATEMENT

The original contributions presented in the study are included in the article/**Supplementary Material**; further inquiries can be directed to the corresponding authors.

## AUTHOR CONTRIBUTIONS

JL, Q-ML, and Y-NY contributed to the synthesis and inhibitory activity evaluation. DX, LL, M-YL, J-PL, and Y-Z contributed to the characterization and analysis of <sup>1</sup>H NMR, <sup>13</sup>C NMR, and MS. ZX, NF, and CL supervised the work and prepared the manuscript.

## FUNDING

This work was financially supported by the Department of Education of Guangdong Province (Nos. 2019KZDXM035, 2021KTSCX135, and 2021KCXTD044) and Special Funds for the Cultivation of Guangdong College Students' Scientific and Technological Innovation ("Climbing Program" Special Funds, pdjh 2021a0504 and pdjh 2022b0532).

## SUPPLEMENTARY MATERIAL

The Supplementary Material for this article can be found online at: <https://www.frontiersin.org/articles/10.3389/fchem.2022.928295/full#supplementary-material>



## REFERENCES

- Al-Salahi, R., Ahmad, R., Anouar, E., Iwana Nor Azman, N. I., Marzouk, M., and Abuelizz, H. A. (2018). 3-Benzyl(phenethyl)-2-thioxobenzo[g]quinazolines as a New Class of Potent  $\alpha$ -glucosidase Inhibitors: Synthesis and Molecular Docking Study. *Future Med. Chem.* 10, 1889–1905. doi:10.4155/fmc-2018-0141
- Álvarez, R., Gajate, C., Puebla, P., Mollinedo, F., Medarde, M., and Peláez, R. (2018). Substitution at the Indole 3 Position Yields Highly Potent Indolecambretastatins against Human Tumor Cells. *Eur. J. Med. Chem.* 158, 167–183. doi:10.1016/j.ejmech.2018.08.078
- Asadollahi-Baboli, M., and Dehnavi, S. (2018). Docking and QSAR Analysis of Tetracyclic Oxindole Derivatives as  $\alpha$ -glucosidase Inhibitors. *Comput. Biol. Chem.* 76, 283–292. doi:10.1016/j.compbiolchem.2018.07.019
- Bao, W., Wang, J.-Q., Xu, X.-T., Zhang, B.-H., Liu, W.-T., Lei, L.-S., et al. (2018). Copper-catalyzed Cyclization of 2-cyanobenzaldehydes and 2-isocyanoacetates: an Efficient Strategy for the Synthesis of Substituted 1-aminoisoquinolines. *Chem. Commun.* 54, 8194–8197. doi:10.1039/c8cc04733b
- Chaudhry, F., Naureen, S., Ashraf, M., Al-Rashida, M., Jahan, B., Munawar, M. A., et al. (2019). Imidazole-pyrazole Hybrids: Synthesis, Characterization and *In Vitro* Bioevaluation against  $\alpha$ -glucosidase Enzyme with Molecular Docking Studies. *Bioorg. Chem.* 82, 267–273. doi:10.1016/j.bioorg.2018.10.047
- Dan, W.-J., Zhang, Q., Zhang, F., Wang, W.-W., and Gao, J.-M. (2019). Benzonate Derivatives of Acetophenone as Potent  $\alpha$ -glucosidase Inhibitors: Synthesis, Structure-Activity Relationship and Mechanism. *J. Enzyme Inhibition Med. Chem.* 34, 937–945. doi:10.1080/14756366.2019.1604519
- Deng, X. Y., Ke, J. J., Zheng, Y. Y., Li, D. L., Zhang, K., Zheng, X., et al. (2022). Synthesis and Bioactivities Evaluation of Oleanolic Acid Oxime Ester Derivatives as  $\alpha$ -glucosidase and  $\alpha$ -amylase Inhibitors. *J. Enzyme Inhib. Med. Chem.* 37, 451–461. doi:10.1080/14756366.2021.2018682
- Gollapalli, M., Taha, M., Javid, M. T., Almandil, N. B., Rahim, F., Wadood, A., et al. (2019). Synthesis of Benzothiazole Derivatives as a Potent  $\alpha$ -glucosidase Inhibitor. *Bioorg. Chem.* 85, 33–48. doi:10.1016/j.bioorg.2018.12.021
- Hu, C. M., Wang, W. J., Ye, Y. N., Kang, Y., Lin, J., Wu, P. P., et al. (2021). Novel Cinnamic Acid Magnolol Derivatives as Potent  $\alpha$ -glucosidase and  $\alpha$ -amylase Inhibitors: Synthesis, *In Vitro* and *In Silico* Studies. *Bioorgan. Chem.* 116, 105435. doi:10.1016/j.bioorg.2021.105291
- Huang, Y., Zhang, B., Li, J., Liu, H., Zhang, Y., Yang, Z., et al. (2019). Design, Synthesis, Biological Evaluation and Docking Study of Novel Indole-2-Amide as Anti-inflammatory Agents with Dual Inhibition of COX and 5-LOX. *Eur. J. Med. Chem.* 180, 41–50. doi:10.1016/j.ejmech.2019.07.004
- Johnson, B. M., Shu, Y.-Z., Zhuo, X., and Meanwell, N. A. (2020). Metabolic and Pharmaceutical Aspects of Fluorinated Compounds. *J. Med. Chem.* 63, 6315–6386. doi:10.1021/acs.jmedchem.9b01877
- Kasturi, S. P., Surarapu, S., Uppalanchi, S., Dwivedi, S., Yogeewari, P., Sigalappali, D. K., et al. (2018). Synthesis, Molecular Modeling and Evaluation of  $\alpha$ -glucosidase Inhibition Activity of 3,4-dihydroxy Piperidines. *Eur. J. Med. Chem.* 150, 39–52. doi:10.1016/j.ejmech.2018.02.072
- Khan, M., Yousaf, M., Wadood, A., Junaid, M., Ashraf, M., Alam, U., et al. (2014). Discovery of Novel Oxindole Derivatives as Potent  $\alpha$ -glucosidase Inhibitors. *Bioorg. Med. Chem.* 22, 3441–3448. doi:10.1016/j.bmc.2014.04.033
- Leong, S. W., Awin, T., Mohd Faudzi, S. M., Maulidiani, M., Shaari, K., and Abas, F. (2019). Synthesis and Biological Evaluation of Asymmetrical Diarylpentanoids as Antiinflammatory, Anti- $\alpha$ -glucosidase, and Antioxidant Agents. *Med. Chem. Res.* 28, 2002–2009. doi:10.1007/s00044-019-02430-5
- Mendieta-Moctezuma, A., Rugerio-Escalona, C., Villa-Ruano, N., Gutierrez, R. U., Jiménez-Montejo, F. E., Fragoso-Vázquez, M. J., et al. (2019). Synthesis and Biological Evaluation of Novel Chromonyl Enaminones as  $\alpha$ -glucosidase Inhibitors. *Med. Chem. Res.* 28, 831–848. doi:10.1007/s00044-019-02320-w
- Prachumrat, P., Kobkeathawin, T., Ruanwas, P., Boonnak, N., Laphookhieo, S., Kassim, M. B., et al. (2018). Synthesis, Crystal Structure, Antioxidant, and  $\alpha$ -Glucosidase Inhibitory Activities of Methoxy-Substituted Benzohydrazide Derivatives. *Crystallogr. Rep.* 63, 405–411. doi:10.1134/s1063774518030227
- Proença, C., Freitas, M., Ribeiro, D., Oliveira, E. F. T., Sousa, J. L. C., Tomé, S. M., et al. (2017).  $\alpha$ -Glucosidase Inhibition by Flavonoids: an *In Vitro* and *In Silico* Structure-Activity Relationship Study. *J. Enzyme Inhibition Med. Chem.* 32, 1216–1228. doi:10.1080/14756366.2017.1368503
- Proença, C., Freitas, M., Ribeiro, D., Sousa, J. L. C., Carvalho, F., Silva, A. M. S., et al. (2018). Inhibition of Protein Tyrosine Phosphatase 1B by Flavonoids: A Structure - Activity Relationship Study. *Food Chem. Toxicol.* 111, 474–481. doi:10.1016/j.fct.2017.11.039
- Proença, C., Freitas, M., Ribeiro, D., Tomé, S. M., Oliveira, E. F. T., Viegas, M. F., et al. (2019). Evaluation of a Flavonoids Library for Inhibition of Pancreatic  $\alpha$ -amylase towards a Structure-Activity Relationship. *J. Enzyme Inhibition Med. Chem.* 34, 577–588. doi:10.1080/14756366.2018.1558221
- Qamar, R., Saeed, A., Saeed, M., Shah, B. H., Ashraf, Z., Abbas, Q., et al. (2018). Synthesis and Enzyme Inhibitory Kinetics of Some Novel 3-(substituted Benzoyl)-2-Thioxoimidazolidin-4-One Derivatives as  $\alpha$ -glucosidase/ $\alpha$ -amylase Inhibitors. *Med. Chem. Res.* 27, 1528–1537. doi:10.1007/s00044-018-2170-4
- Rama Krishna, B., Ramakrishna, S., Rajendra, S., Madhusudana, K., and Mallavadhani, U. V. (2019). Synthesis of Some Novel Orsellinates and Lecanoric Acid Related Depsides as  $\alpha$ -glucosidase Inhibitors. *J. Asian Nat. Prod. Res.* 21, 1013–1027. doi:10.1080/10286020.2018.1490274
- Rocha, S., Sousa, A., Ribeiro, D., Correia, C. M., Silva, V. L. M., Santos, C. M. M., et al. (2019). A Study towards Drug Discovery for the Management of Type 2 Diabetes Mellitus through Inhibition of the Carbohydrate-Hydrolyzing Enzymes  $\alpha$ -amylase and  $\alpha$ -glucosidase by Chalcone Derivatives. *Food Funct.* 10, 5510–5520. doi:10.1039/C9FO01298B
- Santos, C. M. M., Freitas, M., and Fernandes, E. (2018). A Comprehensive Review on Xanthone Derivatives as  $\alpha$ -glucosidase Inhibitors. *Eur. J. Med. Chem.* 157, 1460–1479. doi:10.1016/j.ejmech.2018.07.073
- Settyapalli, T., Chunduri, V. R., Maddineni, A. K., Begari, N., Kotha, P., Chippada, A. R., et al. (2019). Design, Synthesis, *In Silico* Docking Studies and Biological Evaluation of Novel Quinoxaline-Hydrazide Hydrazone-1,2,3-Triazole Hybrids as  $\alpha$ -glucosidase Inhibitors and Antioxidants. *New J. Chem.* 43, 15435–15452. doi:10.1039/c9nj02580d
- Shah, S., ArshiaJavaid, K., Zafar, H., Mohammed Khan, K., Khalil, R., et al. (2018). Synthesis, and *In Vitro* and *In Silico*  $\alpha$ -Glucosidase Inhibitory Studies of 5-Chloro-2-Aryl Benzo[d]thiazoles. *Bioorg. Chem.* 78, 269–279. doi:10.1016/j.bioorg.2018.02.013
- Sonia, R., Daniela, R., Eduarda, F., and Marisa, F. (2019). Meet Our Editorial Board Member. *Curr. Med. Chem.* 26, 1–64. doi:10.2174/092986732601190314143611
- Spasov, A. A., Babkov, D. A., Osipov, D. V., Klochkov, V. G., Pripleskaya, D. R., Demidov, M. R., et al. (2019). Synthesis, *In Vitro* and *In Vivo* Evaluation of 2-Aryl-4h-Chromene and 3-Aryl-1h-Benzo[f]chromene Derivatives as Novel  $\alpha$ -glucosidase Inhibitors. *Bioorg. Med. Chem. Lett.* 29, 119–123. doi:10.1016/j.bmlc.2018.10.018
- Taha, M., Imran, S., Rahim, F., Wadood, A., and Khan, K. M. (2018b). Oxindole Based Oxadiazole Hybrid Analogs: Novel  $\alpha$ -glucosidase Inhibitors. *Bioorg. Chem.* 76, 273–280. doi:10.1016/j.bioorg.2017.12.001
- Taha, M., Ismail, N. H., Imran, S., Wadood, A., Rahim, F., Ali, M., et al. (2015). Novel Quinoline Derivatives as Potent *In Vitro*  $\alpha$ -glucosidase Inhibitors: *In Silico* Studies and SAR Predictions. *Med. Chem. Commun.* 6, 1826–1836. doi:10.1007/s00044-019-02430-510.1039/c5md00280j
- Taha, M., Shah, S. A. A., Afifi, M., Imran, S., Sultan, S., Rahim, F., et al. (2018a). Synthesis,  $\alpha$ -glucosidase Inhibition and Molecular Docking Study of Coumarin Based Derivatives. *Bioorg. Chem.* 77, 586–592. doi:10.1016/j.bioorg.2018.01.033
- Wang, G.-c., Peng, Y.-p., Xie, Z.-z., Wang, J., and Chen, M. (2017). Synthesis,  $\alpha$ -glucosidase Inhibition and Molecular Docking Studies of Novel Thiazolidine-2,4-Dione or Rhodanine Derivatives. *Med. Chem. Commun.* 8, 1477–1484. doi:10.1039/C7MD00173H
- Wang, M.-Y., Cheng, X.-C., Chen, X.-B., Li, Y., Zang, L.-L., Duan, Y.-Q., et al. (2018). Synthesis and Biological Evaluation of novelN-Aryl- $\omega$ -(benzoazol-2-Yl)-Sulfanyalkanamides as Dual Inhibitors of  $\alpha$ -glucosidase and Protein Tyrosine Phosphatase 1B. *Chem. Biol. Drug Des.* 92, 1647–1656. doi:10.1111/cbdd.13331
- Wu, P.-P., Zhang, B.-J., Cui, X.-P., Yang, Y., Jiang, Z.-Y., Zhou, Z.-H., et al. (2017). Synthesis and Biological Evaluation of Novel Ursolic Acid Analogues as Potential  $\alpha$ -glucosidase Inhibitors. *Sci. Rep.* 7, 45578. doi:10.1038/srep45578
- Wu, P.-P., Zhang, K., Lu, Y.-J., He, P., and Zhao, S.-Q. (2014). *In Vitro* and *In Vivo* Evaluation of the Antidiabetic Activity of Ursolic Acid Derivatives. *Eur. J. Med. Chem.* 80, 502–508. doi:10.1016/j.ejmech.2014.04.073
- Xu, X.-T., Mou, X.-Q., Xi, Q.-M., Liu, W.-T., Liu, W.-F., Sheng, Z.-J., et al. (2016). Anti-inflammatory Activity Effect of 2-Substituted-1,4,5,6-

- Tetrahydrocyclopenta[b]pyrrole on TPA-Induced Skin Inflammation in Mice. *Bioorg. Med. Chem. Lett.* 26, 5334–5339. doi:10.1016/j.bmcl.2016.09.034
- Xu, X. T., Deng, X. Y., Chen, J., Liang, Q. M., Zhang, K., Li, D. L., et al. (2019). Synthesis and Biological Evaluation of Coumarin Derivatives as  $\alpha$ -glucosidase Inhibitors. *Eur. J. Med. Chem.* 189, 112013. doi:10.1016/j.ejmech.2019.112013
- Yang, C., Yu, Y., Sun, W., and Xia, C. (2014). Indole Derivatives Inhibited the Formation of Bacterial Biofilm and Modulated Ca<sup>2+</sup> Efflux in Diatom. *Mar. Pollut. Bull.* 88, 62–69. doi:10.1016/j.marpolbul.2014.09.027
- Ye, G.-J., Lan, T., Huang, Z.-X., Cheng, X.-N., Cai, C.-Y., Ding, S.-M., et al. (2019). Design and Synthesis of Novel Xanthone-Triazole Derivatives as Potential Antidiabetic Agents:  $\alpha$ -Glucosidase Inhibition and Glucose Uptake Promotion. *Eur. J. Med. Chem.* 177, 362–373. doi:10.1016/j.ejmech.2019.05.045
- Zhong, Y., Yu, L., He, Q., Zhu, Q., Zhang, C., Cui, X., et al. (2019). Bifunctional Hybrid Enzyme-Catalytic Metal Organic Framework Reactors for  $\alpha$ -Glucosidase Inhibitor Screening. *ACS Appl. Mat. Interfaces* 11, 32769–32777. doi:10.1021/acsami.9b11754

**Conflict of Interest:** The authors declare that the research was conducted in the absence of any commercial or financial relationships that could be construed as a potential conflict of interest.

**Publisher's Note:** All claims expressed in this article are solely those of the authors and do not necessarily represent those of their affiliated organizations, or those of the publisher, the editors, and the reviewers. Any product that may be evaluated in this article, or claim that may be made by its manufacturer, is not guaranteed or endorsed by the publisher.

Copyright © 2022 Lin, Liang, Ye, Xiao, Lu, Li, Li, Zhang, Xiong, Feng and Li. This is an open-access article distributed under the terms of the Creative Commons Attribution License (CC BY). The use, distribution or reproduction in other forums is permitted, provided the original author(s) and the copyright owner(s) are credited and that the original publication in this journal is cited, in accordance with accepted academic practice. No use, distribution or reproduction is permitted which does not comply with these terms.